

Search for Multitrack Nucleon Decay

S. Seidel,^(2,12) R. M. Bionta,⁽¹⁰⁾ G. Blewitt,⁽⁴⁾ C. B. Bratton,⁽⁵⁾ D. Casper,^(2,12) A. Ciocio,⁽¹²⁾ R. Claus,⁽¹²⁾ S. T. Dye,⁽⁶⁾ S. Errede,⁽⁹⁾ G. W. Foster,⁽¹⁴⁾ W. Gajewski,⁽²⁾ K. S. Ganezer,⁽¹⁾ M. Goldhaber,⁽³⁾ T. J. Haines,⁽¹⁵⁾ T. W. Jones,⁽⁷⁾ D. Kielczewska,^(1,8) W. R. Kropp,⁽¹⁾ J. G. Learned,⁽⁶⁾ J. M. LoSecco,⁽¹¹⁾ J. Matthews,⁽²⁾ H. S. Park,⁽¹⁰⁾ L. Price,⁽¹⁾ F. Reines,⁽¹⁾ J. Schultz,⁽¹⁾ E. Shumard,⁽¹³⁾ D. Sinclair,⁽²⁾ H. W. Sobel,⁽¹⁾ J. L. Stone,⁽¹²⁾ L. Sulak,⁽¹²⁾ R. Svoboda,⁽¹⁾ G. Thornton,⁽²⁾ J. C. van der Velde,⁽²⁾ and C. Wuest⁽¹⁰⁾

⁽¹⁾The University of California, Irvine, Irvine, California 92717

⁽²⁾The University of Michigan, Ann Arbor, Michigan 48109

⁽³⁾Brookhaven National Laboratory, Upton, New York 11973

⁽⁴⁾California Institute of Technology, Pasadena, California 91125

⁽⁵⁾Cleveland State University, Cleveland, Ohio 44115

⁽⁶⁾The University of Hawaii, Honolulu, Hawaii 96822

⁽⁷⁾University College, London WC1E 6BT, United Kingdom

⁽⁸⁾Warsaw University, Warsaw, Poland

⁽⁹⁾The University of Illinois, Urbana, Illinois 61801

⁽¹⁰⁾Lawrence Livermore Laboratory, Livermore, California 94720

⁽¹¹⁾The University of Notre Dame, Notre Dame, Indiana 46556

⁽¹²⁾Boston University, Boston, Massachusetts 02215

⁽¹³⁾AT&T Bell Laboratories, Murray Hill, New Jersey 07974

⁽¹⁴⁾Fermi National Accelerator Laboratory, Batavia, Illinois 60510

⁽¹⁵⁾The University of Maryland, College Park, Maryland 20742

(Received 21 April 1988)

We report new limits on the nucleon lifetime obtained with the Irvine-Michigan-Brookhaven water Cherenkov detector. Techniques in track fitting, particle identification, and invariant-mass reconstruction provide information about multitrack events which leads to a significant reduction in background for most decay modes. Data obtained during the initial 417-day run and during the subsequent 69-day run with enhanced light collection are discussed. A background subtraction is made, yielding 90%-confidence-level lower bounds on the nucleon partial lifetime per branching fraction in the range $(0.6-46.0) \times 10^{31}$ yr for 23 decay channels.

PACS numbers: 13.30.Ce

Previously reported results^{1,2} of nucleon-decay searches indicate that decay modes which were initially anticipated by many to dominate the reaction, such as $p \rightarrow e^+ \pi^0$, have no significant excess of candidates above background. Consequently, efforts have been made to search for nucleon decay via alternative channels. The difficulty of identifying these channels is in many cases greater because of the fact that more than two visible tracks or a neutrino occur in the final state. To better distinguish candidates for these decay modes, tracking and particle-identification techniques have been developed by some groups.

The Irvine-Michigan-Brookhaven (IMB) detector³ is a rectangular 8-kton water Cherenkov calorimeter located at a depth of 1580 m of water equivalent (mwe). It is used here to search for nucleon decay to a lepton and a fully reconstructable meson. Contained event vertices are determined from the timing and topology of the photomultiplier tubes (PMT's) triggered, after an initial requirement has been placed upon the number of PMT's triggered. The 401 contained events taken during the initial 417-day run⁴ are combined with 57 contained events

recorded during the subsequent 69 live days⁵ when light-collection enhancement devices⁶ were in place. Using a 3300-metric-ton fiducial volume, the exposure is 4400 metric ton years. The resulting sample of contained events is consistent in rate, energy spectrum, and positional and directional distributions with predictions from models of atmospheric neutrino interactions.

Once each event's vertex has been located,² its topology is determined with a two-stage process. First, all effects of detector geometry are removed. The response of each PMT is corrected for light attenuation, angle-dependent response, and variations in wall density of photocathode. Consequently, the event appears as it would in a detector of isotropic response centered on the vertex. Next, the detector is scanned with a cone centered near the vertex and having half-angle 42° , the Cherenkov angle for relativistic particles. The direction of the event's primary track is taken to be the direction of the cone which intercepts the PMT's having the maximum corrected total photoelectron count. Track 1 is assigned an energy equal to the calibrated pulse height of those PMT's. Primary-track PMT's are then ignored,

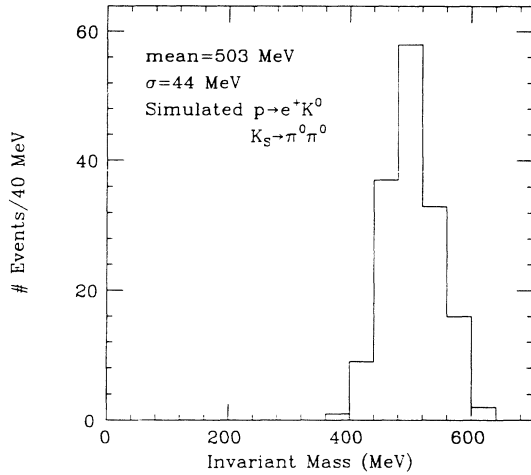


FIG. 1. The reconstructed K^0 invariant mass from simulated events.

and the procedure is iterated until all tracks in the event have been found. A timing cut eliminates scattered light from consideration until reconstruction is complete, at which time the light's equivalent energy is distributed among all tracks. The energy of regions claimed by overlapping tracks is partitioned among the tracks according to the amount of prompt radiation in their non-overlapped regions. The resolution for locating single 500-MeV showering tracks with this method is 5° .

Track recognition makes possible two independent particle-identification procedures—invariant-mass analysis and shower-pattern analysis. When results from both procedures consistent with nucleon decay agree for all tracks considered in an event, the event is called a candidate. Having two methods for track identification provides a powerful discriminating factor against background. All two- and three-track events are considered. Initially the tracks are assigned all combinations of the

TABLE I. Candidate-event-selection requirements. E_c is visible energy, P_{max} is the maximum allowed momentum.

Decay mode	Total E_c (MeV)	Track 1 E_c (MeV)	Track 2 E_c (MeV)	R
$n \rightarrow \nu\rho^0$	150–700	100–500	60–250	0–5
$p \rightarrow \mu^+\rho^0$	150–700	100–500	60–250	0–5
$n \rightarrow \nu\eta^0$	500–750	250–600	100–400	0–3.5
$n \rightarrow \nu\omega^0$	650–950	300–550	250–500	0–2
$p \rightarrow \mu^+\omega^0$	650–950	300–550	250–500	0–2
$p \rightarrow \nu\rho^+$	350–650	200–550	60–350	0–4
$n \rightarrow \mu^+\rho^-$	350–650	200–550	60–350	0–4
$n \rightarrow \mu^-\rho^+$	350–650	200–550	60–350	0–4
$p \rightarrow \gamma e^+$	800–1000	350–700	300–600	0–2.5
$p \rightarrow e^+\pi^0$	800–1100	350–700	300–600	0–2.5
$n \rightarrow e^-\pi^+$	550–900	350–600	100–550	0–4
$n \rightarrow e^+\pi^-$	550–900	350–600	100–550	0–4
$p \rightarrow \gamma\mu^+$	550–900	250–650	100–500	0–4
$p \rightarrow \pi^0\mu^+$	550–900	250–650	100–500	0–4
$n \rightarrow \mu^-\pi^+$	300–600	150–350	60–300	0–3
$n \rightarrow \mu^+\pi^-$	300–600	150–350	60–300	0–3

Decay mode	Total E_c (MeV)	Track 1 E_c (MeV)	Track 2 E_c (MeV)	Track 3 E_c (MeV)	Incl. angle (deg)	P_{max} (MeV)
$p \rightarrow \mu^+\eta^0$	550–900	250–500	125–350	25–250	80–180	600
$p \rightarrow \mu^+K^0$					80–180	
$p \rightarrow e^+\omega^0$	750–1100	275–600	200–475	75–350	120–180	425
$p \rightarrow e^+\eta^0$					80–180	
$p \rightarrow e^+K^0$					60–140	
$n \rightarrow e^+\rho^-$	500–1000	225–475	100–375	65–275	80–180	750
$n \rightarrow e^-\rho^+$					80–180	

Meson	Allowed mass (MeV)
K^0	400–600
η^0	430–670
ω^0	620–920
ρ^\pm	630–910

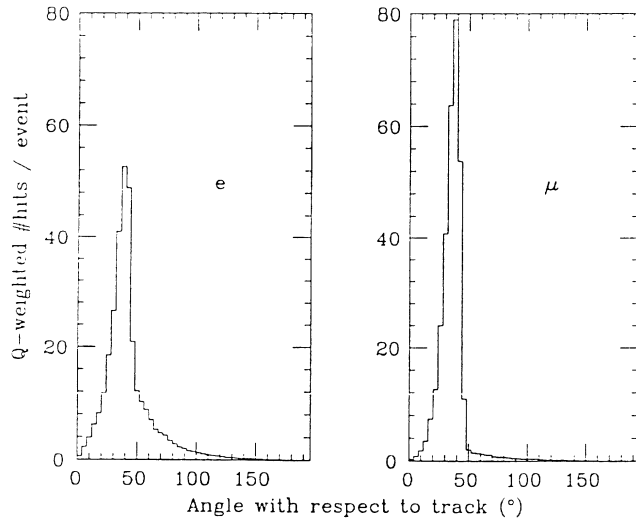


FIG. 2. The energy-weighted angular distribution of light from a simulated electron and muon of visible energy approximately 350 MeV.

identities γ , e , π , and μ which preserve the spin and charge of the decaying nucleon. The overlapping photons from a π^0 decay are treated as a single track. Each track's total energy is computed from its visible energy (E_c) and hypothesized mass. In the case of two-track events, we look for evidence of either a two-body nucleon decay or a decay of the nucleon into a neutrino or a muon below Cherenkov threshold and a heavy meson. The invariant mass of the pair is required to be consistent with that of the nucleon or the heavy meson. The residual momentum must lie below a value P_{\max} , defined as the range of Fermi motion plus resolution smearing. For nucleons, P_{\max} is 350 MeV. In the case of three-track events, we require that the total invariant mass be consistent with that of a nucleon. We require that the mass of the nonleptonic pair be consistent with that of a K^0 , η^0 , ω^0 , or ρ^\pm . We constrain the residual momentum to lie below a value P_{\max} as above. Loose requirements are also made on the total E_c , the E_c of individual tracks, the meson product opening angle, and, in the two-track case, the ratio R of track energies. Figure 1 shows the resolution obtainable on the K^0 mass during the initial run as an illustration of the precision of the technique. Table I summarizes kinematical requirements for all decay modes. Decay-mode identification efficiencies include meson branching fractions and range from the few-percent level to 70%.

Showering and nonshowering particles are distinguished by their light deposition patterns. For tracks of visible energy between 100 and 600 MeV, we simulate energy-weighted PMT hit distributions (where the PMT angle is measured with respect to the reconstructed track) for pairs of average showering and nonshowering particles of the same visible energy. Showering particles

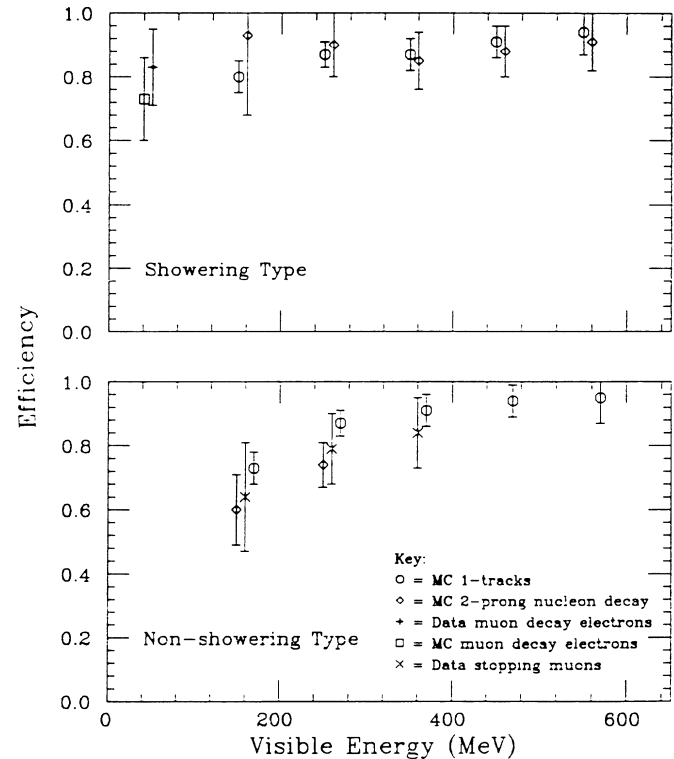


FIG. 3. The particle-identification efficiency for (e) showering and (μ) nonshowering particles.

are characterized in these distributions by tails at angles larger than the Cherenkov angle; nonshowering particles emit almost all of their light at 42° . Figure 2 shows, as an example of typical shower distributions used, the histograms for simulated $E_c = 350$ MeV electrons and muons. Particle identification is made if the number of hits a track generates exceeds a fixed minimum value. The hit distributions of tracks in the data are compared via χ^2 with the paradigm distributions appropriate to their visible energy. The tracks are identified with the particle type which produces the lower χ^2 value. It is possible in some cases to identify overlapping tracks. Efficiencies for the correct identification of nonoverlapping tracks range from 65% for 100 MeV (visible energy) nonshowering particles to >90% for 500-MeV showering particles. They are summarized in Fig. 3

The only significant background to nucleon decay is atmospheric neutrino interaction within the detector. The background simulation technique has been described elsewhere.² To minimize statistical error, background samples are simulated to represent about an order of magnitude more live time than the data represent. Detection efficiencies are determined on a channel by channel basis by filtering large samples of simulated nucleon-decay events.

Seven events from the data satisfy all requirements of nucleon-decay candidates for at least one of 23 decay

TABLE II. Numbers of candidates, expected background, and 90%-confidence-level lifetime lower limits. Systematic errors in the expected background are estimated by our comparing differences in the results of the simulation based upon input from a variety of bubble-chamber experiments. τ is the total lifetime and B is the branching fraction into the mode listed.

Decay mode	No. of candidates	Expected background	τ/B (10^{31} yr)
$n \rightarrow \nu \rho^0$	0	$0.5 \pm 0.2 \pm 0.2$	1.9
$p \rightarrow \mu^+ \rho^0$	0	$0.5 \pm 0.2 \pm 0.2$	3.0
$n \rightarrow \nu \eta^0$	3	$2.1 \pm 0.4 \pm 0.5$	1.6
$n \rightarrow \nu \omega^0$	2	$1.3 \pm 0.3 \pm 0.3$	0.6
$p \rightarrow \mu^+ \omega^0$	2	$1.3 \pm 0.3 \pm 0.6$	1.0
$p \rightarrow \nu \rho^+$	1	$1.1 \pm 0.3 \pm 0.1$	1.3
$n \rightarrow \mu^+ \rho^-$	1	$1.1 \pm 0.3 \pm 0.1$	1.1
$n \rightarrow \mu^- \rho^+$	1	$1.1 \pm 0.3 \pm 0.1$	0.7
$p \rightarrow \gamma e^+$	0	$0.6 \pm 0.2 \pm 0.1$	46
$p \rightarrow \gamma \mu^+$	0	$0.5 \pm 0.2 \pm 0.1$	38
$p \rightarrow e^+ \pi^0$	0	$0.6 \pm 0.2 \pm 0.1$	31
$n \rightarrow e^+ \pi^-$	0	$1.6 \pm 0.3 \pm 0.4$	10
$n \rightarrow e^- \pi^+$	0	$1.6 \pm 0.3 \pm 0.4$	6.5
$p \rightarrow \pi^0 \mu^+$	0	$0.5 \pm 0.2 \pm 0.1$	27
$n \rightarrow \mu^+ \pi^-$	0	$0.5 \pm 0.2 \pm 0.1$	6.3
$n \rightarrow \mu^- \pi^+$	0	$0.5 \pm 0.2 \pm 0.1$	4.9
$p \rightarrow e^+ \eta^0$	0	$0.6 \pm 0.2 \pm 0.1$	10
$p \rightarrow \mu^+ \eta^0$	1	$1.5 \pm 0.3 \pm 0.1$	3.4
$p \rightarrow e^+ \omega^0$	1	$1.0 \pm 0.3 \pm 0.2$	2.6
$p \rightarrow e^+ K^0$	0	$1.8 \pm 0.3 \pm 0.4$	7.0
$n \rightarrow e^+ \rho^-$	2	$4.1 \pm 0.5 \pm 0.7$	3.8
$n \rightarrow e^- \rho^+$	2	$4.1 \pm 0.5 \pm 0.7$	6.2
$p \rightarrow \mu^+ K^0$	3	$2.5 \pm 0.4 \pm 0.5$	1.9

modes considered. This is a significant reduction in candidates from the 28 which were found for these channels by previous analysis of 417-day data alone. Three of the events are candidates for only one decay channel. In two cases, the masses of both the nucleon and its product meson are reconstructed. In four, the mass of the meson alone is recovered. The remaining event is consistent with being both ω^0 and nucleon depending upon its classification as a two- or three-track event. The average candidate event has its reconstructed meson mass and, where applicable, its nucleon mass within 1.25σ of their nominal values. All candidates' masses are below 2.5σ

of their nominal values. Candidate vertices are distributed uniformly in the detector fiducial volume. No single decay mode dominates the production of candidates. No enhancement above background is apparent for any mode. Background subtracted 90%-confidence-level lower bounds on the nucleon partial lifetime per branching fraction are obtained by determining the 90%-confidence-level number of candidates for each channel in the presence of the expected number of background events for that mode, under the constraint that the number of background events cannot be greater than the number of candidates observed. The subtraction yields bounds on the nucleon partial lifetime per branching fraction in the range $0.6\text{--}46 \times 10^{31}$ yr. Table II summarizes the results.

We are grateful for the continued support of the Morton-Thiokol Company which operates the Fairport Harbor mine. This work was supported in part by the U.S. Department of Energy.

¹T. Kajita *et al.*, J. Phys. Soc. Jpn. **55**, 711 (1986); M. R. Krishnaswamy *et al.*, Nuovo Cimento **9C**, 167 (1986); G. Battistoni *et al.*, Nuovo Cimento **9C**, 182 (1986); J. Bartelt *et al.*, Phys. Rev. D **36**, 1990 (1987); C. Berger *et al.*, Orsay Report No. LAL 88-28, 1988 (to be published); H. Meyer, in *Proceedings of the Twelfth International Conference on Neutrino Physics and Astrophysics, Sendai, Japan, 1986*, edited by T. Kitagaki and H. Yuta (World Scientific, Singapore, 1986).

²H. S. Park *et al.*, Phys. Rev. Lett. **54**, 22-25 (1985).

³R. M. Bionta *et al.*, Phys. Rev. Lett. **51**, 27 (1983); R. M. Bionta *et al.*, in Proceedings of the Fermilab Workshop on Calorimeter Calibration, Fermi National Accelerator Laboratory, Batavia, Illinois, 1983 (unpublished).

⁴H. S. Park *et al.*, in *Proceedings of the Twentieth Rencontre de Moriond: Perspectives of Electroweak Interactions*, edited by J. Tran Thanh Van (Editions Frontières, Gif-sur-Yvette, France, 1985); G. Blewitt *et al.*, Phys. Rev. Lett. **55**, 2114-2117 (1985); T. J. Haines *et al.*, Phys. Rev. Lett. **57**, 1986-1989 (1986).

⁵S. C. Seidel, Ph.D. thesis, The University of Michigan, 1987 (unpublished).

⁶R. Claus *et al.*, Nucl. Instr. Methods Phys. Res., Sect. A **261**, 540-542 (1987).